The Development of Solid Electrochemical Deposition (SED)

E.Z. Tang*, T. H. Etsell and D.G. Ivey

Department of Chemical and Materials Engineering,
University of Alberta, Edmonton, AB, Canada T6G 2G6

ABSTRACT

The interfacing of thin film vapor deposition technologies and solid state electrochemistry has led to the recent development of solid electrochemical deposition (SED). Studies have shown that SED processes have fundamental similarities in terms of mass and charge transport through the solids for further deposition. The emergence of SED techniques for fabricating fully dense thin-film ceramic components, and creating intimate contact between solid electrolytes and electrodes, has made possible the successful fabrication of solid state ionic devices, such as solid oxide fuel cells and sensors. Furthermore, SED also holds the promise of being used as an experimental tool to determine the physical properties of different solid state ionic materials of fundamental and practical importance.

1. INTRODUCTION

There are two types of conductivity in nature: electronic and ionic. The first does not involve material transport while the second does. Mass and charge transport associated with ionic conduction in condensed matter (solids) have been known since the 19th century /1/. In 1933, Wagner /2/ combined the foregoing concepts of mass and charge transport in solids, and published a detailed analysis of the parabolic tarnishing of metals in aggressive environments. He assumed that (a) transport of neutral species was negligible compared to that of ions and electronic carriers; (b) all the charged carriers migrated with Einstein-type mobilities under the combined influences of chemical potential gradients and electric fields. In this way, he was able to transform the problem of parabolic scaling of metals to one of diffusional transport in a solid electrochemical medium. The ionic and electronic transport within solids suggested by Wagner's tarnishing theory has two sets of implications.

First of all, ionic and electronic transport within solid state ionic (SSI) materials permit material transport through solids in a controlled manner. The prospect of controlling corrosion by controlling reactant transport through the scale products initially generated much excitement in corrosion engineering circles. However, because of various complicating factors /3/, this optimism was somewhat misguided. Material transport through tarnishing products can hardly be controlled under actual corrosion conditions, and only a limited number of metal scaling systems important to modern technology strictly conform to the conditions required by Wagner's tarnishing theory.

Secondly, since materials transport through SSI materials involves both ionic and electronic current flow, conversion between electrical and chemical energy in a solid electrochemical cell is possible. By choosing appropriate SSI materials, with appropriate interfaces, a simple external electrical circuit can be used to study, monitor or convert the chemical characteristics of various neighboring phases separated by a solid electrolyte. In the past 60 years, this second principle from Wagner's electrochemical tarnishing theory has been combined with those from semiconductor physics to build up a new field, solid state electrochemistry /4/. This field evolved to deal with solids in which combined ionic and electronic transport can take place to allow transformation from chemical energy to electrical energy (or vice versa). Meanwhile, a variety of important SSI materials were discovered, and numerous energy conversion applications based on the energy transformation capability of SSI materials have been identified since the "energy crisis" in the 1970s. Many SSI devices /5/, such as sensors, fuel cells and batteries, were developed. In all of these applications, the solid electrolyte element can be expected to perform according to Wagner's tarnishing theory /6/.

* Current address: Fuel Cell Division, Global Thermoelectric, Inc., Calgary, AB, Canada T2C 2L8

In spite of the great promise SSI devices offer, few of them have been commercialized today. At present, the key technical challenge is development of reliable and cost-efficient techniques to synthesize SSI materials to serve as solid electrodes and electrolytes /7/. On the other hand, SSI materials are not used in isolation, but in an electrochemical system and must be in contact with each other. The response of SSI materials in SSI devices is highly related to the interface characteristics, which fix the external electrical conditions (electric potential and current density) and the external chemical conditions (chemical potential). Thus, the solid electrode/electrolyte interfaces must possess high ionic and electronic mobility. Development of fabrication techniques to improve the interfaces assumes real significance /8/.

Recently, solid electrochemical deposition (SED) techniques have been developed to meet the above mentioned fabrication challenges. In general, SED takes advantage of not only energy transformation but also material transport itself during ionic and electronic transport in solids to form desired products. This brought Wagner's electrochemical tarnishing theory back to the initial application of controlling material transport for solid product formation. But this time in SED, the material transport and product formation are under well-controlled thermodynamic and kinetic conditions.

Research and development in this field indicated that SED is promising with a wide range of potential technological applications for SSI devices. Furthermore, SED also holds the promise for use as an experimental tool to determine the defect structure and transport parameters of different SSI materials of fundamental and practical importance /9/.

The purpose of this review paper is to give a unified approach to two separately developed SED techniques, electrochemical vapor deposition (EVD) /10/ and polarized electrochemical vapor deposition (PEVD) /11/. After a discussion of their common theoretical aspects in the next section, their principles and applications will be discussed separately. It is not our intention to include all previous investigations of SED. Emphasis will be placed on numerous significant applications of both SED techniques, for solid state ionic devices as well as for product physical property studies, in the hope of promoting future research in this area.

2. SED FUNDAMENTALS

Solid electrochemical deposition is a modified form of conventional chemical vapor deposition (CVD). Figure 1 compares SED with conventional CVD. Briefly, in an SED process, at least one reactant (A) is transported from the source side of a solid phase (E) to the sink side under well-controlled thermodynamic and kinetic conditions. At the sink side surface, which is exposed to the vapor phase reactant (B), reaction occurs to form the solid compound deposit (D). Further growth of deposit (D) into a thin film with desired thickness in an SED process also relies on solid-state transport of reactant (A) through the deposited thin film (D) to react with reactant (B) from the vapor phase.

The reason that reactant (A) can be transported

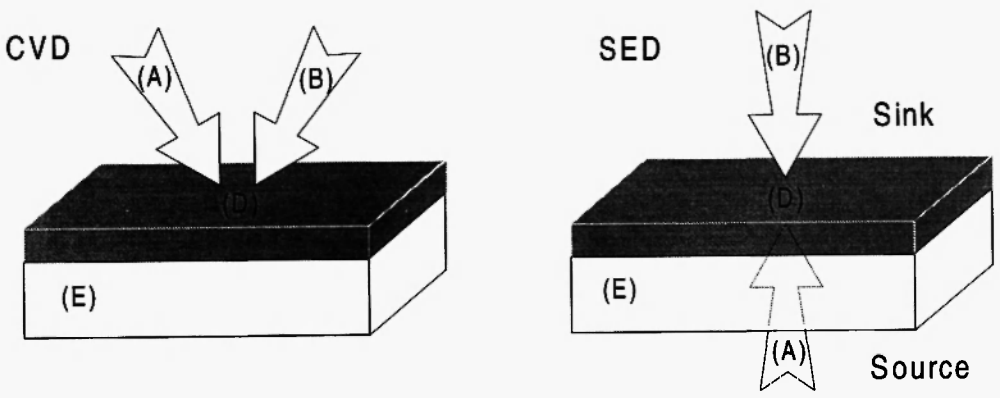

Fig. 1: Comparison of SED and CVD processes

through solid phase (E) and the deposited phase (D) is because (E) and (D) are solid state ionic materials /12/, in which the ionic state of reactant (A) is mobile. According to Wagner's tarnishing theory, reactant (A) will be transported as a combination of corresponding ionic, A^{z+} (or A^{z-}), and electronic carriers, electrons e (or holes h), under the mixed influences of chemical potential gradients and electric fields in the solid (E). Unlike the chemical reaction of vapor phase reactants (A) and (B) to form deposit (D) in CVD, in SED, the reaction of the solid state transported reactant (A) and the vapor phase reactant (B) to form deposit (D) is electrochemical in nature. Thus, the process is called solid electrochemical deposition. The immediate advantage is the reaction can only occur at an electrochemically active area instead of a catalytically active area. Thus, the reaction and deposition in SED take place only on the substrate, not on reactor walls, as there are no vapor phase reactions as may occur in CVD. The deposits in SED are usually uniform and fully dense, due to the fact that the electrochemical potential gradient is the driving force for electrochemical reaction and film growth. Thus, where the film is the thinnest, the driving force is the greatest. Through this self-leveling effect, very uniform films are expected.

The way electronic carriers are transported to deposits (D) in an SED system distinguishes the two kinds of SED processes developed so far. In electrochemical vapor deposition (EVD), the electronic carriers flow with ionic carriers through the solid phase (E) to the deposited product (D). In polarized electrochemical vapor deposition (PEVD), a solid electrochemical cell is set up and the electronic carriers flow separately to the deposit product (D) through an external electrical circuit mainly under the influence of an applied dc potential. The difference between EVD and PEVD is schematically shown in Figure 2.

In EVD, the solid (E) can be any kind of solid state ionic material (either a predominantly ionic or predominantly electronic conductor). As long as the major mobile ionic species is A^{z+} (or A^{z-}), the driving force for reactant (A) transport through the solid phase (E), and deposit (D) for further reaction and growth, is the chemical potential difference between the two isolated compartments, i.e., the source and sink side of the solid phases. At the source side, the chemical potential of the reactant (A) is usually maintained constant. At the sink side, the chemical potential of reactant (A) is fixed by the EVD reactions. The driving force for EVD is the Gibbs free energy of the overall EVD redox reactions, or the chemical potential difference of the solid state transported reactant (A) between the source and sink sides.

In PEVD, the solid state ionic material (E) is an exclusive ionic conductor for A^{z+} (or A^{z-}). It serves as the solid electrolyte in a solid electrochemical cell, i.e. it is connected through an external electrical circuit with a dc electrical source by two electronic conducting electrodes at both the sink and source sides of solid electrolyte (E). Consequently, the driving force for reactant (A) transport through solid electrolyte (E) is controlled by an applied dc electrical potential, instead of relying only on the chemical potential difference of

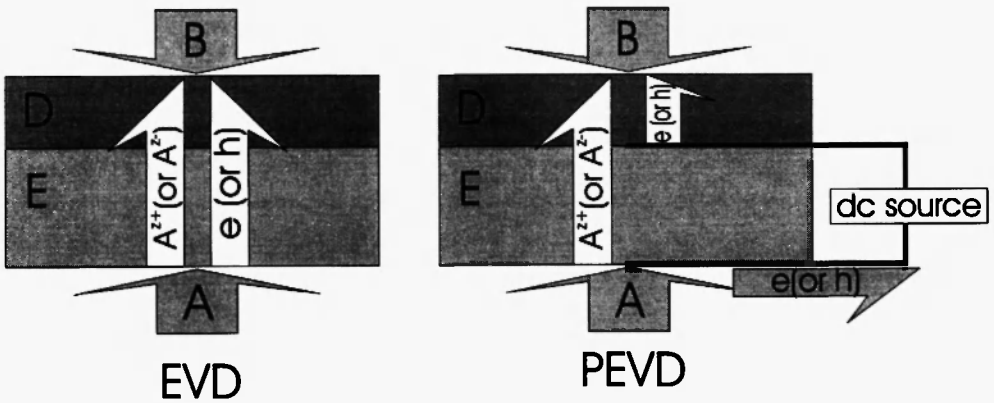

Fig. 2: Comparison of EVD and PEVD processes

reactant (A) over solid phase (E) as in EVD. In this way, isolation between source and sink sides is not necessary. Nevertheless, the transport of reactant (A) through deposit (D) for further growth in PEVD bears the same mechanism as in EVD. However, PEVD offers more control of the chemical potential gradient through deposit (D) than EVD.

In short, the characteristic feature of SED is that deposit (D) growth is driven by the presence of a chemical potential gradient of reactant (A) across deposit (D). This gradient drives the transport of reactant (A) in the form of ionic and electronic charged carriers through deposit (D). The growth of deposit (D) resembles Wagner's theory, governing the growth of an oxide scale on metal, and is parabolic in nature. Unlike the initial applications of Wagner's theory in corrosion, solid transport of reactant in SED is under well-controlled thermodynamic and kinetic conditions, through vapor phase control in EVD, and through dc electrical potential control via a solid electrochemical cell in PEVD.

3. OPEN CIRCUIT SED – ELECTROCHEMICAL VAPOR DEPOSITION (EVD)

The desire of achieving thin and pore-free yttria stabilized zirconia (YSZ) films as an electrolyte over a porous electrode (cathode) to reduce the ohmic resistance of solid oxide fuel cells (SOFCs) led to the development of a new vapor deposition method. Electrochemical vapor deposition (EVD) was first introduced by Isenberg at the Westinghouse R&D center in Pittsburgh, Pennsylvania in the late 1970s /10,13/. Later, both university and industrial research laboratories in the US, Japan and the Netherlands continued to work to improve the EVD process. This work has led to numerous patents over the last ten years /14-16/.

The principles of the EVD process, to deposit a thin layer of YSZ on a porous cathode of SOFCs, have been outlined extensively in the literature /17-21/. The actual process is a CVD/EVD two-stage process as schematically shown in Figure 3. Briefly, it consists of passing specific amounts of halides containing the required cations ($ZrCl_4$ and YCl_3) over one side of a porous substrate; the halides are chosen for their relatively high vapor pressures. Oxygen and/or steam at a given activity is passed on the other side of the substrate.

The first stage is a counter-diffusion chemical vapor deposition process. In this stage of the reaction, molecular diffusion of oxygen, steam and metal halides ($ZrCl_4$ and YCl_3) occurs through the pores in the substrate, and they react to fill the pores with the desired oxides according to the chemical reactions,

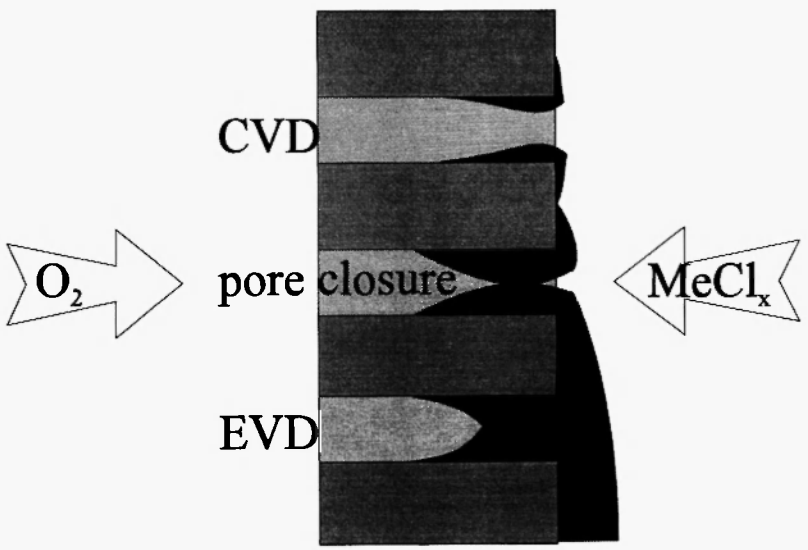

Fig. 3: CVD/EVD process to deposit a YSZ thin film on a porous substrate.

$$ZrCl_4 + 2H_2O \rightarrow ZrO_2 + 4HCl$$
$$2YCl_3 + 3H_2O \rightarrow Y_2O_3 + 6HCl \quad (1)$$

The processing pressure, temperature, type of halides, and their respective flows are chosen so that the reaction is thermodynamically favored. After this counter-diffusion CVD process, all the pores in the substrate are sealed by YSZ to form two separate compartments that serve as source and sink sides of the substrate /22/.

The actual EVD process occurs in the second stage /10/. The gradient in oxygen potential that exists across the deposited YSZ (in the pores), between the halide (sink) side and the oxygen (source) side, causes solid-state electrochemical transport of the ionic species (O^{2-}) and an electronic species (e) to maintain electroneutrality. At the sink side, both charged species react with the reactants in the gas phase electrochemically to form the desired products,

$$ZrCl_4 + 2O^{2-} - 4e^- \rightarrow ZrO_2 + 2Cl_2$$
$$2YCl_3 + 3O^{2-} - 6e^- \rightarrow Y_2O_3 + 3Cl_2 \quad (2)$$

and the product continues to grow as a film over the substrate.

Thermodynamically, the driving force for growth in EVD is the electrochemical reaction and formation of the product. This creates an oxygen chemical potential difference between the two sides of the substrate, which is sealed after the first stage of counter-diffusion chemical vapor deposition.

Kinetically, the rate-limiting step in an electrochemical reaction is the same as that in a chemical reaction, i.e., the slowest step controls the reaction as well as the deposition rate. Thus, all major kinetic effects should be considered, such as pore diffusion, charge transfer reactions and bulk diffusion. In the past few years several groups have investigated the kinetics of this EVD process. Both linear /10/ and parabolic /21,23/ growth rates were observed. To investigate this discrepancy, Lin *et al.* /24/ developed a model which showed that there is always a transition behavior for any EVD process on porous substrates. At the beginning of the EVD phase, diffusion of the oxygen source reactant through the substrate pores is the rate-limiting step for layer growth. When the deposition layer thickness is larger than the so-called transition thickness, bulk diffusion through the film plays the dominant role in the film growth process /25/. This model further indicated /24/ that transition thickness depends on the deposition conditions such as substrate characteristics, experimental temperature and pressure.

Recently, critical evaluation of the literature data was given by Dekker *et al.* /26/. In their study, all reported parabolic rate constants in EVD studies were gathered and presented in an Arrhenius plot, which strongly supported the argument that bulk diffusion of electrons in the product layer controls product growth in an EVD process. This study also indicated that increasing the processing temperature would increase the growth rate, because electronic transport inside the product is a thermally activated process /27/. Calculation shows that by increasing the temperature from 1273 K to 1473 K, the growth rate can increase more than six-fold /23/. According to the diffusion coefficients for electronic charged carriers in YSZ /28,29/, a 6 μm/hour growth rate can be obtained for 10 mol% YSZ at 1300 K /30/, which has been experimentally verified by Carolan and Michaels /23/. However, in the case of pore diffusion limiting growth, a lower deposition rate of only 1 to 2 μm/hour was reported /31/.

In order to eliminate other reaction limiting steps and to obtain the maximum deposition rate, parameters such as temperature, pressure, etc. in an EVD process are chosen so that electronic transport inside the product thin film layer is the rate-limiting step. Thus, the deposition is usually conducted at low pressures ($\leq 10^{-4}$ atm) and high temperatures ($\geq$1273 K) to obtain fast surface reactions. Under these conditions, the solid-state electrochemical transport of minority carriers (electrons in this case) is the slowest step and controls the deposition rate /9/.

Besides the high deposition rate; conducting the EVD process in the solid state transport limiting regime is critical to growing a uniform and gas tight layer. Because the electrochemical reaction is limited by solid state transport, growth will be fastest in the shortest transport directions. Consequently, a fully dense and uniform layer of YSZ results.

Two types of surface morphology have been reported in the EVD growth of YSZ: a faceted type and a "cauliflower type" of surface /23, 30/. The difference

in morphology can be explained by a change in relative rates of film growth and surface reconstruction, or possibly due to the thermodynamic instability of a surface species at high temperatures /32/.

In order to lower the operating temperature of SOFCs, EVD has received much attention over the past decade or so as a technique for the deposition of several other oxides or doping with other dopants than yttrium to stabilize zirconia resulting in lower resistance solid electrolytes for SOFCs. Other than doping with yttrium to stabilize zirconia, EVD has also been utilized to deposit zirconia doped with ytterbium or co-doped with yttrium and ytterbium /20/.

An EVD process of depositing CeO_2 on dense Y_2O_3-doped CeO_2 substrates was demonstrated for the fabrication of a two-layer composite electrolyte /33-35/. In their studies, $CeCl_3$ vapor was used as the source of cerium. Unlike CVD/EVD processes for depositing YSZ on porous substrates, the mass transport processes through different solid phases in the deposited thin film and the substrate should be taken into account in this case. The same group also showed the possibility of using a liquid $CeCl_3$ precursor to deposit CeO_2 on a Gd_2O_3-doped CeO_2 substrate /36/. The process was named electrochemical liquid deposition (ELD), and is similar to EVD, as CVD is similar to chemical liquid deposition (CLD). This presents the possibility of expanding solid electrochemical deposition further to transport reactants through the solids and react with a reactant in phases other than the vapor phase.

EVD has also been used to grow perovskite interconnection materials for fabricating tubular SOFCs at Westinghouse /37/. Generally, the interconnection material used in SOFCs must have a high electronic conductivity, be gas tight, and be stable in both oxidizing and reducing ambients. The current common choice is Mg-doped lanthanum chromite ($LaCrO_3$), which is a p-type semiconductor with a small contribution of oxygen ion conductivity /38/. Early studies by Isenberg /39/ on the EVD deposition of doped $LaCrO_3$ indicated a problem with the incorporation of dopants into the film. This problem is partially solved by adding an excess of the corresponding chloride /40/. However, a high temperature is required for a reasonable deposition rate. Pal and Singhal /41/ have observed a growth rate constant of 1.8×10^{-9} cm^2s^{-1} at 1600K for 2 mol% Mg-doped $LaCrO_3$. The activation energy for oxygen ion diffusion is estimated to be 0.8 eV, which is in the range of activation energies for oxygen ion diffusion in perovskite materials /42/. This again confirms Wagner's tarnishing theory that minority charge carriers control the growth of EVD products. In the case of electronic conducting $LaCrO_3$, growth is controlled by transporting oxygen ions through the deposit by a vacancy mechanism /37/.

Another application of EVD in SOFC fabrication was published in one of Isenberg's patents for fabricating Ni/YSZ cermet anodes using EVD methods /43/. Isenberg reported that the resistance to sintering was improved in this kind of anode, but the details are not clear. The EVD process has also been applied to deposit YSZ on a Ru anode of an SOFC /44/. It is reported that the YSZ grew along the surface of the Ru metal particles, and that Ru and YSZ were in good contact. The SOFC with this kind of cermet anode demonstrate a good anode stability and very high power generation density. However, the mechanism was not discussed in the paper.

Besides applications for SOFCs, the synthesis of thin dense films of solid state ionic materials on porous substrates is also of great interest for other SSI devices. More recent applications of EVD grown layers include oxygen sensors, electrocatalytic reactors and oxygen separation membranes. Particularly in the last mentioned application, the thickness of the membrane layer is of importance. Where the bulk electrochemical diffusion of oxygen ions through the layer is the rate limiting step in the separation process, membrane layers should be as thin as possible to obtain a maximum oxygen permeation rate. By means of EVD, gas tight layers of a YSZ film /45/ with thicknesses as small as 0.2-0.5 μm can be obtained on a coarse porous α-alumina substrate. EVD has become a key technology for depositing these kinds of layers. In another study by Brinkman and Burggraaf /46/, EVD was applied to deposit a thin, dense layer of a zirconia/yttria/terbia solid solution (ZYT) on porous ceramic substrates as ceramic membranes for oxygen separation. Oxygen permeation values of the order of 10^{-8} $mol/cm^2\bullet s$ have been achieved in the temperature range 900 to 1000°C under a large oxygen partial pressure gradient.

In conclusion, the characteristic features of the EVD technique are as follows.

(a) Uniform and gas tight compound layers with thicknesses as small as 0.2-0.5 μm can be obtained /45/, and the deposited films adhere well to substrates.

(b) A single-step process can be used to grow films up to hundreds of microns thick, unlike sol-gel processes which require multiple dip-coatings followed by several heating steps to synthesize films of a reasonable thickness (a few microns).

(c) Deposition temperatures are typically on the order of 1100 to 1200°C for many materials, while typical sintering temperatures are 1500 to 1600°C /39/.

Several other techniques, such as tape casting /47,48/, radio frequency sputtering /49,50/, plasma spraying /51/, and low temperature CVD /52,53/ have been investigated in parallel. None of these have equaled the performance of electrochemical vapor deposition. Thus, EVD has become a key technology for the aforementioned applications.

4. CLOSED CIRCUIT SED – POLARIZED ELECTROCHEMICAL VAPOR DEPOSITION (PEVD)

The need to cover a porous Pt working electrode with a thin layer of auxiliary phase (Na_2CO_3) for the Type III potentiometric CO_2 gas sensor led to the development of another method of solid electrochemical deposition – polarized electrochemical vapor deposition (PEVD), which was initiated by Tang *et al.* in 1995 /11/.

Weppner /54/ has classified potentiometric sensors into three types, in which type III is the state-of-the-art design for detecting gaseous oxides (CO, CO_2, NO, NO_2 and SO_2) /55/. The topic was reviewed recently by Yamazoe and Miura /56/. In general, type III potentiometric gaseous oxide sensors utilize an auxiliary phase (such as Na_2CO_3 for CO_2) to provide a unique relationship between the variations of the partial pressure of the gaseous oxides in ambient atmosphere and the chemical potential of the mobile ionic carriers in the solid electrolyte. As a result, some good fast ionic conductors, such as Na^+-β"-alumina /57/ and Nasicon ($Na_3Zr_2Si_2PO_{12}$) /58/ can be used as solid electrolytes for these sensors. Thus, the auxiliary phases have vital importance for type III potentiometric gaseous oxide sensors /59/. Recently, a gas sensing model for type III potentiometric gaseous oxide sensors was studied by Tang *et al.* /60/, and six geometric criteria for the auxiliary phase at the sensor's porous working electrode were proposed. The auxiliary phase should be a thin layer which covers and is in intimate contact with both the metallic electrode and the solid electrolyte. However, depositing a thin film on a very irregularly shaped substrate with a high aspect ratio, as found for porous metallic working electrodes in potentiometric sensors, poses significant difficulties. PEVD was developed in our laboratory to meet the challenge. A typical PEVD setup for Na_2CO_3 auxiliary phase deposition is schematically shown in Figure 4.

Basically, the PEVD process takes advantage of the solid electrolyte, Na^+-β"-alumina, which can transport sodium reactant in the ionic state (Na^+) under an electrochemical potential gradient. This gradient in PEVD is mainly created by an external dc electrical potential in a solid electrochemical cell. During a PEVD process, a chemical redox reaction takes place at both the source and sink electrodes. At the source side, Na_2CO_3 gives up sodium ions and electrons according to the electrochemical reaction

$$Na_2CO_3 \rightarrow 2Na^+ + 2e^- + CO_2 + \tfrac{1}{2}O_2 \qquad (3)$$

Sodium ions and electrons migrate separately through the solid electrolyte and external electrical circuit, respectively. At the sink side, sodium ions combine with electrons and react with CO_2 and O_2 in the gas phase to form the Na_2CO_3 auxiliary phase, according to the following electrochemical reaction.

$$2Na^+ + 2e^- + CO_2 + \tfrac{1}{2}O_2 \rightarrow Na_2CO_3 \qquad (4)$$

The overall reaction for this solid electrochemical cell is

$$(\text{source})Na_2CO_3 \rightarrow Na_2CO_3(\text{sink}) \qquad (5)$$

This overall reaction indicates that materials, e.g., Na_2CO_3, can be transported through a solid phase under an applied dc electrical potential gradient in a solid electrochemical cell.

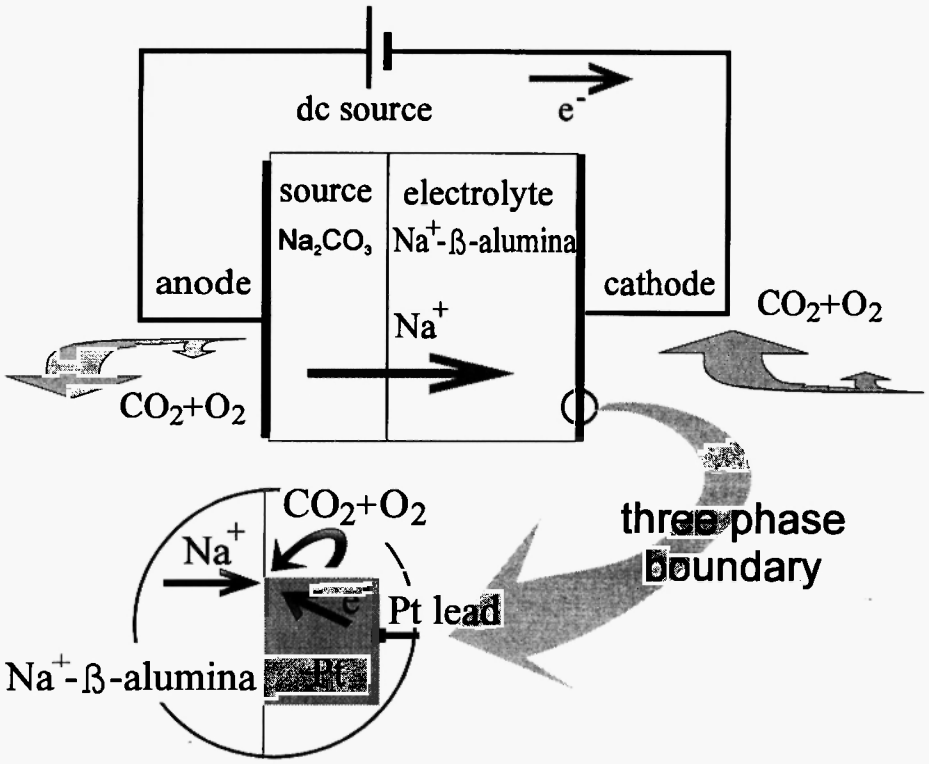

Fig. 4: PEVD process for Na_2CO_3 auxiliary phase deposition at the working electrode of a potentiometric CO_2 sensor.

Utilization of solid electrochemical cells is one of the most significant advantages of the PEVD technique, since controlling and monitoring of the deposition process are easy to realize. By connecting a simple external electrical circuit to a PEVD system, the chemical redox reaction in PEVD is easily monitored and controlled by the electrical current and applied potential, respectively /11/.

First of all, because at least one reactant needs to be transported from the source to the sink electrode through the solid electrolyte of a solid electrochemical cell in a PEVD process, the chemical redox reaction rate is proportional to the rate of ionic transport through the solid electrolyte. Consequently, Faraday's law relates the rate of PEVD reaction and product growth to the electrical current passed through the external electrical circuit. Furthermore, taking into account the evolution of the cell with time, the amount of reaction product is easy to monitor during PEVD.

Secondly, because the thermodynamic driving force for both the chemical redox reaction and ionic transport is mainly supplied by the applied external dc electrical potential in PEVD, adjusting the applied potential controls the chemical potential difference of the solid-transported reactant across the deposited product over a wider range than EVD. Consequently, the applied potential controls the chemical redox reaction rate in a PEVD system when diffusion through the product is the rate-limiting step. On the other hand, because the thermodynamic driving force for the PEVD reaction is not based on chemical potential difference of solid-transported reactant between the sink and source side, isolation of both sides is not necessary. This provides a great practical advantage of PEVD over EVD.

Experimental results indicate that PEVD deposited auxiliary phases are not only in intimate contact with the solid electrolyte and Pt thick film, but are also thin and uniformly cover the substrate surface. This unique growth behavior of the deposit during PEVD has been investigated /61/. As in EVD, PEVD product growth is also very much dependent on it own physical properties

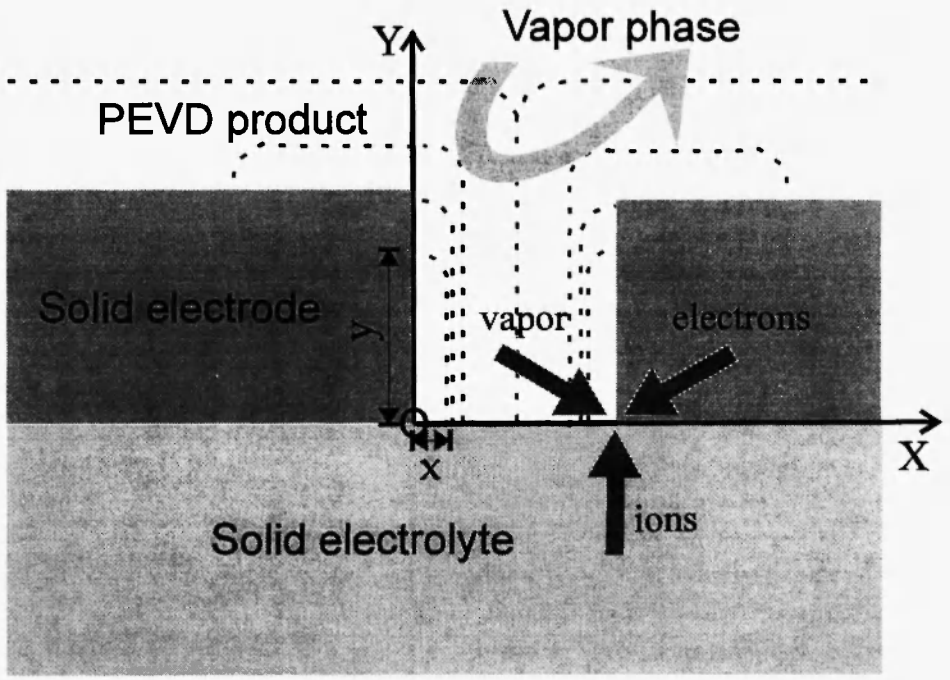

Fig. 5: PEVD growth on electrically shorted surfaces.

(ionic and electronic conductivity). The growth behavior of a PEVD product phase is schematically shown in Figure 5. After nucleation at a three phase boundary (gas/Pt electrode/Na^+-β^n-alumina electrolyte), the initial growth of PEVD product Na_2CO_3 may occur along two kinds of electrically shorted surfaces. Along the ionically shorted surface of the solid electrolyte, growth will be limited by transport of electrons through the product. Along the electronically shorted surface of the metallic electrode, growth will be limited by transport of ions through the product. According to experimental results for Na_2CO_3 growth /11/, ionic conductivity in Na_2CO_3 is much larger than electronic conductivity. Consequently, the Na_2CO_3 auxiliary phase exhibits preferred growth along the electronically shorted surface to cover the entire Pt electrode with a thin layer /11/.

After the electrically shorted surfaces have been covered, further growth to increase the product thin film thickness is much like the growth in EVD. Growth at this stage is limited by minority charge carrier transport through the product phase, and the parabolic law is followed. Finally, a fully dense PEVD product of uniform thickness is obtained. Compared with all the commonly used methods for auxiliary phase deposition, the superiority of PEVD is obvious, since the Na_2CO_3 auxiliary phase can be deposited in a well-controlled manner *in-situ* at the working electrode to meet all the geometric criteria /60/.

Improvement of the geometric structure of the working electrode by a well-controlled in-situ PEVD process benefits the performance of a CO_2 sensor in many aspects, including sensitivity, stability, selectivity and sensor response behavior /62,63/. In a recent paper /64/, the response and recovery times of a CO_2 potentiometric sensor were studied as a function of the amount of the Na_2CO_3 auxiliary phase deposited at the working electrode controlled by PEVD. It was found that the response behavior of the sensor is dependent on the thickness of the auxiliary phase and the aspect ratio of the working electrode. In an optimized condition, a potentiometric CO_2 sensor can be obtained with a response time of less than 1 min and a recovery time of less than 3 min, for CO_2 partial pressures varying from 30 to 300 ppm at the working electrode.

Furthermore, the unique growth behavior of PEVD

made it the best process to improve solid electrode/ electrolyte interfaces for other solid state ionic devices, such as solid oxide fuel cells and batteries. In general, an inherent disadvantage of SSI devices is that interfacial contact is often poor /65,66/; unlike liquids, there is no "wetting" of the contacted surface of the solid components. Therefore, when a solid electrode is employed in conjunction with a solid electrolyte, in most devices electrode polarization is almost inevitable. Currently, this is one of the toughest technical problems faced by SSI devices. Thus, developing new fabrication techniques to improve the contact characteristics at the interface is of great practical importance.

Recently, experimental results in our laboratory have indicated that PEVD is a very promising technique to fabricate cermet anodes /67/ for SOFCs. PEVD for YSZ thin film deposition to cover porous metallic electrode surfaces is similar to that in an EVD process. However, in PEVD, a dc potential is applied through an external electrical circuit between the anode and cathode. This dc potential provides the driving force to transport oxygen through the solid electrolyte. Compared with the EVD technique, since the major driving force in PEVD is supplied by the electrical potential, it is not necessary to seal the anode side from the cathode side during PEVD. This is of great practical importance when depositing PEVD cermet anodes for planar SOFCs. Furthermore, the chemical potential of oxygen over the deposited YSZ is more controllable with an applied dc potential, and an optimized growth rate can be obtained through a current and overpotential study. Because of the unique growth behavior of the PEVD process, the ionic conducting product (YSZ) in PEVD is able to cover a high aspect ratio metallic electrode with a very thin layer to form a continuous ionic conducting path while preserving the porous nature as schematically shown in Figure 6.

This cermet anode configuration will reduce the overpotential loss and significantly improve the long-term stability of the anode for the following reasons:

(a) The PEVD YSZ layer, grown from the solid electrolyte along the metallic electrode, will increase the adhesion between the solid electrolyte and metallic electrode.

(b) Continuous ionic and electronic paths in a PEVD cermet anode increase the electrochemically active area, from a two-dimensional interface region between the metallic electrode and solid electrolyte to a three-dimensional surface, without suffering the ohmic conductivity loss encountered in cermet anodes made by the commonly applied slurry coating technique.

(c) With a very thin layer of YSZ, sintering, poisoning and vapor loss of the metallic electrode will be prevented.

(d) Practically, PEVD can be applied to form cermet anodes in-situ, or even be used to repair an anode after a period of SOFC operation.

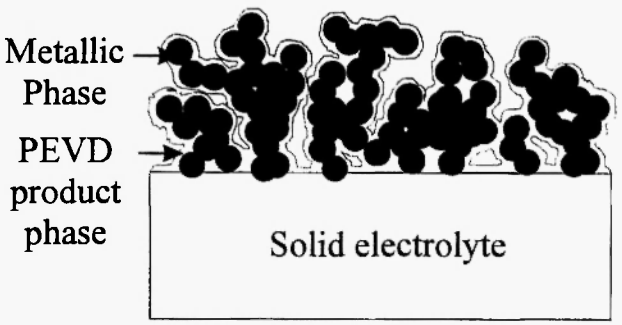

Fig. 6: PEVD cermet anode.

5. UTILIZING SED TO STUDY THE PHYSICAL PROPERTIES OF DEPOSITS

Wagner's tarnishing theory implies that the parabolic scale formation rate constants can be quantitatively related to two basic types of information:

A) Thermodynamic information, such as the free energy of formation for the scale and the partial pressure or activity data for the environment.

B) Electrical property information for the scaling compound, such as electrical conductivity, ionic and electronic transference numbers, and the open circuit emf established over the growing scale.

This suggests the possibility of using the growth behavior of SED products to reveal their physical properties under well-defined thermodynamic conditions in SED processes.

Conventional defect structure and transport property studies of a solid state ionic material generally just give information about the majority species but not the minority species, although the minority species are often vital in controlling critical properties of an SSI material /9/. In SED processes, minority charged carriers control the product growth rate. Thus, by utilizing proper deposition rate measurements, one should be able to calculate solid-state transport properties, such as transport numbers and partial conductivities, of the rate-controlling minority species in SED products as a function of temperature, partial pressure and dopant concentration.

With the aid of microstructural observation of the thickness of the deposited thin film at various deposition times, growth rate constants of EVD products have been reported extensively, according to the following equation under the assumption that bulk diffusion in the growing layer comprises the rate limiting step /26/,

$$L^2 = 2Kt + C \tag{6}$$

where K is the parabolic rate constant, L the film thickness, t the total deposition time, and C a constant of integration.

The parabolic rate constant, K, for YSZ can be expressed as follows /9,68/,

$$K = \frac{RTV_m}{4cF^2} \int_{p_{O_2}'}^{p_{O_2}''} \sigma_e \, d \ln P_{O_2} \tag{7}$$

where R is the gas constant, T is the temperature in Kelvin, V_m is the molar volume of YSZ, c is the total anion charge per equivalent in EVD deposited YSZ, σ_e is the electronic conductivity in EVD deposited YSZ, F is Faraday's constant, and P_{O2}' and P_{O2}'' are the oxygen partial pressures in atm at the sink and source side, respectively. Thus, electronic conductivity of the EVD deposits can be studied under various experimental conditions.

Recently, a critical review of the literature data for EVD YSZ growth at various temperatures was given by Dekker *et al.* /26/. The activation energy for electronic conductivity was obtained via a simple Arrhenius plot. The value of 4.4 eV obtained was close to the previously reported value /69/. A more effective method was suggested by Tanner *et al.* /35/. Their approach consists of using a substrate of variable thickness so that path lengths for diffusion vary spatially and the local film thickness is also a function of position. Rate constants for both the product and substrate can then be determined in a single experiment.

In another investigation, Pal and Singhal /37/ suggested that the relative mobilities of the ionic species in an SSI material can be estimated by placing inert markers over the substrate before deposition, and following the position of the markers as the film grows.

Partial conductivities of the minority species obtained in EVD investigations can not be used quantitatively, since thicknesses estimated from microstructural studies of a number of cross-sectioned samples are not accurate. Thus, accurate determination of growth rates is the key to quantification. PEVD offers a more direct way to study the physical properties of its product by utilizing a solid electrochemical cell. Since currents in a PEVD system can be very precisely measured, reaction rates may be evaluated with high precision /70/. For instance, a current of 1 mA corresponds to the transport of about 10^{-8} equivalents of the mobile ionic reactant per second. The equation for the parabolic rate constant K /71/ is

$$K = \frac{iV_m L}{nzF} \tag{8}$$

where I, V_m, L, n, z and F are the current, the molar volume of the product, the instantaneous thickness of the layer, the stoichiometric number of mobile ionic reactants in the product, the charge number of the mobile ionic reactant and Faraday's constant, respectively. A more direct way is to construct a solid electrochemical cell in a PEVD system with a proper reference electrode. The potential difference between the sink and reference electrode is the resistance overpotential over the product thin film. In this way, the slope of a current-overpotential curve is the partial conduction of the minority charged carrier over the product thickness. Instead of measuring the thickness directly in both these methods, this quantity may be determined by integrating the current when one starts with a clean substrate with no reaction product.

Besides the capability to reveal the minority charged carriers in SED products, SED product growth behavior on electrically shorted surfaces /72/ can be used to study the conductivities of both minority and majority charged carriers along various crystallographic directions /73/.

As schematically shown in Figure 5, the growth rate (or equivalent growth length) of an SED product along ionic conducting surface X will be limited by electron transport in the product phase. The growth distance x can be expressed as

$$x = \left(V_m \sigma_e \Delta G t / F^2\right)^{1/2} \quad (9)$$

where σ_e is the electronic conductivity in the product phase, ΔG is the Gibbs free energy of the reaction, V_m is the molar volume of the product, and t is the time. Along the Y direction, i.e., the surface of the electronic conducting material, the reaction-limiting step is ionic transport in the product phase. The growth distance y can be expressed as

$$y = (4/\pi)(V_m \sigma_i \Delta G t / F^2)^{1/2} \quad (10)$$

where σ_i is the ionic conductivity in the product phase. The ratio of y/x is

$$\frac{y}{x} \approx \frac{1.265\sqrt{\sigma_i}}{\sqrt{\sigma_e}} \quad (11)$$

and is only related to the electronic and ionic conductivity of the PEVD product phase /74/.

Generally speaking, the mechanisms for ionic and electronic conduction in solids are quite different. Ionic conduction is mainly related to crystal structure; electronic conduction is determined by the electronic bandgap, which depends more on the individual properties of the constituent ions /25/. Thus, ionic conductivity in solids is extremely sensitive to crystallographic considerations, whereas electronic conductivity is more isotropic. A product crystal with a preferred ionic conducting crystallographic direction exactly along the electronically shorted surface would grow much faster than the others. According to Eq.(9-11), when an SED product crystal grows on an electronically shorted surface, various crystallographic orientations in the product phase will exhibit a different y/x ratio. In a recent paper, Tang *et al.* suggested a way to use transmission electron microscope (TEM) diffraction to reveal the preferred ionic conducting crystallographic direction in an SED product phase /61/.

Although several possibilities have been proposed so far, application of this novel SED process approach as an experimental and analytical tool to study defect structures and solid-state transport properties of SSI materials is in its infancy.

6. CONCLUSIONS

According to Wagner's electrochemical tarnishing theory, material transport in solids requires transport of both electronic and ionic species. This theory has contributed to the development of numerous solid state ionic devices to transform electrical energy to chemical energy, and vice versa. It also provides the principles of recently developed solid electrochemical deposition techniques, in which well-controlled material transport through solids can be used to form desired products. Analysis of both SED techniques has indicated that electrochemical vapor deposition (EVD) is the best technique to deposit fully dense components of SSI devices; polarized electrochemical vapor deposition (PEVD) is apparently the most suitable technique to improve the solid electrode / electrolyte contact for SSI devices. Furthermore, the "active" use of material transport through the solid by solid electrochemical deposition offers more interesting opportunities not only for forming deposition products but also for studying the physical properties of the products under well-defined thermodynamic and kinetic conditions.

It has been more than 60 years since Wagner's tarnishing theory was developed. The two parallel suggestions of material transport and energy transformation in the theory are integrated, and the newly developed SED techniques will make solid state ionic devices better to serve today's ever-growing energy and environmental demands.

REFERENCES

1. L.W. Strock, *Z. Phys. Chem.*, B25 (1934) 441.
2. C. Wagner, *Z. Phys. Chem.*,B 21, (1933) 25.
3. N.S. Choudhury and J.W. Patterson, *J. Electrochem. Soc.*, 118 (1971) 1389.
4. C. Wagner, in: *Proceedings of the 7th Meeting, Lindau, 1955 (CITCE)*, ed., p.361, Butterworths, London, (1957).
5. O. Tillement, *Solid State Ionics*, 68 (1994) 9.
6. J.W. Patterson, in: *Electrical Conductivity in Ceramics and Glass*, N. M. Tallan, ed., p.453, Marcel Dekker, N.Y. (1974).
7. T. Takahashi, in: *Superionic Solids and Solid Electrolytes*, Materials Sciences Series, A.L. Laskar and S. Chandra, ed. p.1, Academic Press, New York (1989).
8. M. Kleitz, P. Fabry and E. Schouler, in: *Proc. Electrode Processes in Solid State Ionics*, NATO Adv. Study Inst. Ser. C., M. Kleitz and J. Dupuy, eds. p.1, Reidel Publ. Co., Dordrecht, Holland (1975).
9. U.B. Pal, *Solid State Ionics*, 52 (1992) 227.
10. A.O. Isenberg, in: *Proc. Symp. on Electrode Materials and Processes for Energy Conversion and Storage IV*, J. McBreen, S. Mukerjee, and S. Srinivasan, (eds.), p.572, Electrochemical Society Proceeding Series, 77-6, Princeton, NJ, (1977).
11. E. Z. Tang and T. H. Etsell, *Solid State Ionics*, 91 (1996) 213.
12. J. Hladik, in: *Physics of Electrolytes*, J. Hladik, Edit. p. 35, Academic Press, (1972).
13. A.O. Isenberg, *Solid State Ionics*, 3 / 4 (1981) 431.
14. A.O. Isenberg, US Patent 4,490,444 (Dec. 25, 1984).
15. A.O. Isenberg, US Patent 4,582,766 (Apr, 15, 1986).
16. A.O. Isenberg, US Patent 4,728,584 (Mar. 1, 1988).
17. M.F. Carolan and J. N. Michaels, *Solid State Ionics*, 25 (1987) 207.
18. L.G.J. de Haart, Y.S. Lin, K.J. de Vries and A. J. Burggraaf, *J. Eur. Ceram. Soc.*, 8 (1991) 59.
19. G. Dietrich and W. Schäfer, *Int. J. Hydrogen Energy*, 9 (1984) 747.
20. J. Schoonman, J.P. Dekker, J.W. Broers and N.J.Kiwiet, *Solid State Ionics*, 46 (1991) 299.
21. U.B. Pal and S.C. Singhal, *J. Electrochem. Soc.*, 137 (1990) 2937.
22. Y.S. Lin, K.J. de Vries, and A.J. Burggraaf, *J. de Phys., Colloque* C5, 50 (1989) 861.
23. M.F. Carolan and J. N. Michaels, *Solid State Ionics*, 37 (1990) 189.
24. Y.S. Lin, L.G.J. de Haart, K.J. de Vries and A.J. Burggraaf, *J. Electrochem. Soc.*, 137 (1990) 3960.
25. L. Heyne, in: *Solid Electrolytes*, S. Geller, ed., p.169, Springer-Verlag, Berlin (1977).
26. J.P. Dekker, V.E.J. van Dieten and J. Schoonman, *Solid State Ionics*, 51 (1992) 143.
27. J.M. Park and R.N. Blumenthal, *J. Electrochem. Soc.*, 136 (1989) 2867.
28. W. Weppner, *Electrochim. Acta*, 22 (1977) 721.
29. W. Weppner, *J. Solid State Chem.*, 20 (1977) 305.
30. J.P. Dekker, N.J. Kiwiet and J. Schoonman, in: *Solid Oxide Fuel Cells*, S.C. Singhal, ed., p.57, The Electrochemical Society Proceeding Series, Pennington, NJ, 89-11, (1989).
31. Y.S. Lin, L.G.J. de Haart, K.J. de Vries and A.J. Burggraaf, in: *Solid Oxide Fuel Cells*, S.C. Singhal, ed., p.67, The Electrochemical Society Proceeding Series, 89-11, Pennington, NJ (1989).
32. M.F. Carolan and J.N. Michaels, *Solid State Ionics*, 37 (1990) 197.
33. J.F. Jue, J. Jusko and A.V. Virkar, *J. Electrochem. Soc.*, 139 (1992) 2458.
34. C.W. Tanner, J.F. Jue and A.V. Virkar, *J. Electrochem. Soc.*, 140 (1993) 1073.
35. C.W. Tanner and A.V. Virkar, *J. Electrochem. Soc.*, 141 (1994) 1262.
36. C.W. Tanner and A.V. Virkar, *J. Am. Ceram. Soc.*, 77 (1994) 2209.
37. U. B. Pal and S. C. Singhal, *High Temp. Sci.*, 27 (1990) 251.
38. W.J. Weber, C.W. Griffin and J.L. Bates, *J. Am. Ceram. Soc.*, 70 (1987) 265.
39. A.O. Isenberg, *Thin Film Battery/Fuel Cell Power Generating System.* Report ERDA. Contract EY-76-C-03-1197, Westinghouse Electric Corporation, (1978).
40. S.C. Singhal, *Interconnection Material*

Development for Solid Oxide Fuel Cells, DOE contract DE-AC21-84MC21184. Final report (1985).

41. U.B. Pal and S.C. Singhal, in: *Solid Oxide Fuel Cells*, S.C. Singhal, ed., p.41, The Electrochemical Society Proceeding Series, 89-11, Pennington, NJ (1989).
42. T. Ishigaki, S. Yamaguchi, K. Koshio, J. Misuzaki and K. Fueki, *J. Solid State Chem.*, 73 (1988) 179.
43. A.O. Isenberg, Japanese Patent, Application no. S60-269217 (1985).
44. M. Suzuki, H. Sasaki, S. Otoshi, A. Kajimura and M. Ippommatsu, *Solid State Ionics*, 62 (1993) 125.
45. Y.S. Lin, K.J. de Vries, H.W. Brinkman and A.J. Burggraaf, *J. Membrane Sci.*, 66 (1992) 211.
46. H.W. Brinkman and A. J. Burggraaf, *J. Electrochem. Soc.*, 142 (1995) 3851.
47. J.J. Bentzen, J.B. Bilde-Sorensen, B. Kindl and H.W. Poulsen, in: *Proc. of the 5th SSMS on New Materials and Processes*, I.L.H. Hansson and H. Lilholt (eds.), p.149, Copenhagen, (1989).
48. T. Setohuchi, H. Ito, M. Sawano, K. Eguchi and H. Arai, in: *Proceedings of the International Symposium on Solid Oxide Fuel Cell*, O. Yamamoto, M. Dokiya and H. Tagawa, eds., p.105, Science House, Tokyo (1989).
49. J.E. Green, C.E. Wickersham, J.L. Zilko, L.B. Walsh and F.R. Szofran, *J. Vac. Sci. Technol.*, 13 (1976) 72.
50. A. Neglishi, K. Nozaki and T. Ozawa, *Solid State Ionics*, 3 / 4 (1981) 443.
51. H. Hamatani, T. Okada and T. Yoshida, in: *Proceedings of the International Symposium on Solid Oxide Fuel Cells*, O. Yamamoto, M. Dokiya and H. Tagawa, eds., p.119, Science House, Tokyo (1989).
52. Q. Minh Nguyen, C.R. Horne, F. Liu, P.R. Staszak, T.L. Stillwagon and J.J. van Ackeren, in: *Solid Oxide Fuel Cells*, S.C. Singhal, ed., p.307, The Electrochemical Society Proceeding Series, 89-11, Pennington, NJ (1989).
53. P.A. Lessing, L.W. Tai and K.A. Klemm, in: *Solid Oxide Fuel Cells*, S.C. Singhal, ed., p.337, The Electrochemical Society Proceeding Series 89-11, Pennington, NJ, (1989).
54. W. Weppner, *Sensors and Actuators*, 12 (1987) 107.
55. W. Weppner, German Patent DE 2926172C2 (June 28, 1979).
56. N. Yamazoe and N. Miura, *Sensors and Actuators B*, 20 (1994) 252.
57. R. Akila and K.T.Jacob, *Sensors and Actuators*, 16 (1989) 311.
58. S.Yao, Y. Shimizu, N. Miura and N. Yamazoe, *Chem. Lett.*, 1992 (1992) 587.
59. N. Yamazoe and N. Miura, *IEEE Transaction on Components, Packing, and Manufacturing Technology*, Part A, v. 18, n. 2 (1995) 252.
60. E. Z. Tang, T. H. Etsell and D. G. Ivey, *Sensors and Actuators B*, 45 (1997) 21.
61. E.Z. Tang, D.G. Ivey and T.H. Etsell, *Micron*, 29 (1998) 251.
62. N. Miura, S. Yao, Y. Shimizu and N. Yamazeo, *J. Electrochem. Soc.*, 139 (1992) 1384.
63. W.F. Chu, D. Fischer, H. Erdmann, M. Ilgenstein, H. Koppen and V. Leonhard, *Solid State Ionics*, 53-56 (1992) 80.
64. E.Z. Tang, T.H. Etsell and D.G. Ivey, in *Ceramic Sensors III*, H.U.Anderson, M. Liu and N. Yamazoe, (eds.), p.131, The Electrochemical Society Proceeding Series, 96-27, Pennington, NJ (1996).
65. R.M. Dell, in: *Proc. Electrode Processes in Solid State Ionics*, NATO Adv. Study Inst. Ser. C., M. Kleitz and J. Dupuy, (eds.), p.387, D. Reidel Publ. Co., Dordrecht, Holland (1975).
66. M.B. Armand, in: *Polymer Electrolyte Reviews*, J.R. MacCallum and C.A. Vincent (eds.), p.1, Elsevier, Amsterdam (1987).
67. E. Z. Tang, D. G. Ivey and T. H. Etsell, in: *Diffusion Mechanisms in Crystalline Materials*, Y. Mishin, N.E.B. Cowern, C.R.A. Catlow, D. Farkas and G.Vogl, (eds.), p. 539, Material Research Society, Warrendale, PA (1998).
68. P. Kofstad, in: *High Temperature Corrosion*, Elsevier Applied Science, Oxford, (1988) 162.
69. J. M. Park and R. N. Blumenthal, *J. Electrochem. Soc.*, 136 (1989) 2867.
70. H. Rickert, in: *Reactivity of Solids*, 5th Int. Symp., G.M. Schwab, ed., p.214, Elsevier, Amsterdam, (1964).
71. W. Weppner, *Ann. Rev. Mater. Sci.*, 8 (1978) 269.

72. C. Ilschner-Gensch and C. Wagner, *J. Electrochem. Soc.*, 105 (1958) 198.
73. E.Z. Tang, T.H. Etsell and D.G. Ivey, in: *Electrochemically Deposited Thin Films III*, M. Paunovic and D.A. Scherson, (eds.), p.71, The Electrochemical Society Proceeding Series, 96-19, Pennington, NJ, (1996).
74. R.A. Rapp and D.A. Shores, in: *Physicochemical Measurements in Metals Research, part 2,* R.A. Rapp, ed., p. 123, Interscience, New York (1970).